The Ohmic heating of particulates in a lossless medium

Wilkin Tang, Herman Bosman, Y. Y. Lau,[a] and R. M. Gilgenbach
Department of Nuclear Engineering and Radiological Sciences, University of Michigan, Ann Arbor, Michigan 48109-2104

(Received 7 January 2005; accepted 4 April 2005; published online 7 June 2005)

This paper provides a general theory on the Ohmic dissipation of electromagnetic energy by a spherical particulate that is embedded in a lossless medium. The particulate may possess an arbitrary electrical conductivity, and both the medium and the particulate may assume general values of permittivity and permeability. Under the assumption that the wavelength of the electromagnetic field in the medium is large compared with the particulate size, we provide an accurate account of the degree of Ohmic heating by the radio frequency (rf) electric field and by the rf magnetic field of the electromagnetic field. It is found that, in general, heating by the rf magnetic field is dominant whenever $\delta < a$, where δ is the resistive skin depth and a is the radius of the particulate. Analytic scaling laws in the various regimes are derived, from the static case to very high frequency, and for ratios of δ/a ranging from zero to infinity. The calculation is extended to a transient electromagnetic pulse. Also constructed is the loss tangent of the medium, resulting from a distribution of particulates. © *2005 American Institute of Physics*. [DOI: 10.1063/1.1922085]

I. INTRODUCTION

Heating phenomenology is an important topic in science and engineering. Microwave heating has been applied to the sintering of ceramics[1,2] and rubber vulcanization, and has potential uses in the treatment of mineral ores,[3] heating of catalysts[4,5] in chemical reactions, and regeneration of molecular sieves.[6] Elective doping of a substrate is used to enhance the absorption of radiation at a certain wavelength in modern lithographic or processing techniques.[7,8] In high-power microwave components and sources, heating of the contaminants on metallic surfaces and dielectric surfaces is known to cause localized damage.[9,10] Thermal effects in biological systems that are exposed to radiation have been studied for decades.[11,12] In many of these processes, the lowest-level description is through the macroscopic constitutive relations, $\mathbf{D}=\varepsilon\mathbf{E}$, and $\mathbf{B}=\mu\mathbf{H}$, where the imaginary parts in the permittivity ε and in the permeability μ provide a quantitative measure of the electromagnetic energy absorption. These imaginary parts, in many cases, may be considered as due to the particulate absorbers that reside within an otherwise lossless medium.[13]

In this paper, we provide an incisive evaluation of the degree of absorption of the rf electric-field energy and the rf magnetic-field energy by a particulate. In virtually all of the literature on particulate heating, the heatings by the rf electric field and by the rf magnetic field are treated separately and independently.[12–14] If the particulate is assumed to be exposed to a time varying electric field, the electrical polarizability α_E is calculated, where α_E is a measure of the electrical energy absorbed by the particulate in one rf cycle. Alternatively, if the particulate is assumed to be exposed to a time varying magnetic field, this time varying magnetic field induces an electric field within the particulate by Faraday's law. This induced electric field drives an Ohmic current and therefore results in an Ohmic dissipation in the particulate. The magnetic polarizability α_H is then calculated, where α_H is a measure of the rf magnetic energy absorbed by the particulate through this inductive electric field. In the case of a high-frequency field, such as one that resides inside a microwave resonant cavity, one may question whether the heating by the rf electric field or by the rf magnetic field can be treated separately and independently, since the two fields are strongly coupled. In fact, in a resonant microwave cavity, the total-energy contents in these two types of fields are equal, even though there are regions of strong rf magnetic field and regions of strong rf electric field.

Recently, there has been experimental evidence which shows that the heating via the rf magnetic field in a microwave resonant cavity may be dominant, even when the particulates or the medium appears to be nonmagnetic in nature. For example, Dolgashev and Tantawi found that melting of metallic debris inside a high-power rf cavity occurred at the regions of high rf magnetic field.[9] Cheng *et al.* found in their heating experiments that the rf magnetic field might effect a higher heating rate than the rf electric field in a microwave cavity.[2] Our recent work on the heating of surface contaminants and of graphitic impurities inside a high-power microwave window,[10,15] and our ongoing work on the effects of biological cells when exposed to ultrashort electrical pulses,[16] together with the above-mentioned heating experiments, provided a strong impetus to our general study of particulate heating, the results of which are reported in this full-length paper. A specific goal is to resolve the degree of particulate heating by the rf electric field and by the rf magnetic field. The preliminary results of our findings have been reported.[17]

We should mention that the interaction of a particulate with an incident electromagnetic wave had a long history that began with the work of Rayleigh, now under the general term of the Mie scattering.[18] When the electrical permittivity ε_1 of the particulate is complex, the total power absorbed by

[a]Electronic mail: yylau@umich.edu

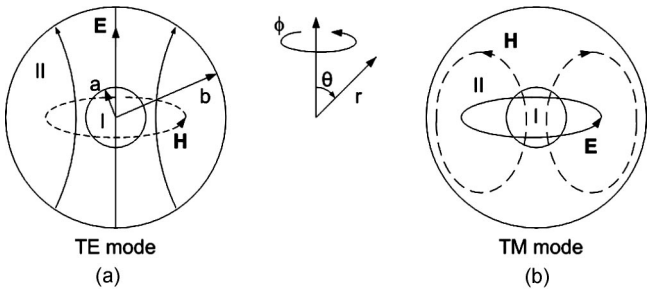

FIG. 1. The geometry and the rf field patterns for (a) the TE_{110} mode and (b) the TM_{110} mode. The mode index (110) refers to variations in r, θ, and ϕ.

the particulate is not easy to obtain, even to this date, because the distribution of the electromagnetic fields within the particulate needs to be numerically calculated in a Mie scattering formalism. Accurate numerical solutions are particularly difficult to obtain when there is a large separation in the three spatial scales: the wavelength λ, the particulate radius a, and the resistive skin depth δ. State-of-the-art eigenmode solvers remain ill equipped to simulate the minuscule perturbing effects of a small particulate, when the skin depth is small compared with the particulate size, which in turn is typically small compared with the size of the resonant cavity. Slater's perturbation techniques also fail in this case.[19]

The difficulties described in the last three sentences are largely overcome in the present paper. When the size of the spherical particulate is small compared with the cavity dimension (of order the wavelength for lowest-order modes), the local electromagnetic field, at the location of that particulate, may be considered as a linear superposition of a transverse-electric (TE) mode and a transverse-magnetic (TM) mode. The power dissipated by that local TE (TM) mode may be accurately calculated by pretending that this spherical particulate is now located at the center of a perfectly conducting spherical cavity that admits a TE (TM) mode of the same amplitude and frequency (Fig. 1). Note that the high degree of symmetry of the latter model allows *exact* solutions to the Maxwell equation for the TE and TM modes, for arbitrary values of a, δ, and λ.[17] Substantial simplification of the results may then be obtained for $a \ll \lambda$, a limit of considerable practical importance. The values of the quality factor Q, for both the TE and TM modes in the perfectly conducting cavity, will become finite if the particulate is lossy. The quality factor Q immediately yields the polarizabilities α_E and α_H, since all of these quantities measure the power dissipated in the particulate.[17] For the general case where the particulate is located off-center of a resonant cavity, α_E and α_H then give the Ohmic dissipation of the local TE and TM modes by the particulate, without the formidable computation of the field distributions within the particulate, in an irregular three-dimensional geometry. Thus, the highly symmetrical model shown in Fig. 1 enables us to calculate the polarizabilities α_E and α_H, fully taking into account the conduction current and displacement current in both the TE and TM modes. The asymptotic forms of these polarizabilities will be presented. They are derived from the general expressions and from simple physical arguments aided by a dimensional analysis.

The general expression of α_E and α_H that we derive also allow an evaluation of the total Ohmic power deposited into the particulate when it is subjected to an electromagnetic pulse of a finite pulse length. The pulse may have a general spectrum. We next calculate the added loss tangent in a medium that is sparsely populated with the particulates. When there is significant Ohmic dissipation in the metallic particulates through the rf magnetic field (as is generally the case when $\delta \ll a$), these lossy metallic particulates in effect lead to an effective complex μ in an otherwise electric medium.[13]

In Sec. II, we use the highly symmetrical model to calculate the electric and magnetic polarizabilities for the TE and TM modes. Section III presents the numerical results and the comparison with the asymptotic expressions in the various regimes. The total energy deposited in the particulate by a finite electromagnetic pulse is presented in Sec. IV. In Sec. V, we calculate the contributions to the loss tangent in a dielectric that results from the embedded, sparsely populated particulates. The concluding remarks are given in Sec. VI. Some details of the derivations are given in the Appendices.

II. THE MODEL

The power absorbed by the particulate in the presence of a TE mode or a TM mode may be calculated exactly in the simple model shown in Fig. 1. We place a homogenous, spherical particulate of radius a at the center of a spherical cavity. The cavity has radius b and its wall is infinitely conducting. In the absence of this particulate, the spherical cavity admits the fundamental transverse-electric TE_{110} mode, which has a maximum rf electric field (and a null rf magnetic field) at the center, as well as the transverse-magnetic TM_{110} mode, which has a maximum rf magnetic field (and a null rf electric field) at the center (Fig. 1). Both the TE mode and TM mode have an infinite quality factor Q since the cavity wall is lossless. [For convenience of discussions, in this paper and in our previous communication,[17] we have defined in Fig. 1, and more generally, the TE mode as the one in which the rf electric field is maximum at the location of the particulate, and the TM mode as the one in which the rf magnetic field is maximum at the location of the particulate. Thus, this designation is the opposite of that given in Ramo *et al.*,[20] who call Fig. 1(a) the TM mode and Fig. 1(b) the TE mode.]

When a small lossy particulate is inserted at the center of this cavity (Fig. 1), the modes are slightly damped. The quality factors become finite, and the eigenmode frequency becomes complex. To evaluate this change in the eigenfrequency, let us use the subscripts 1 and 2 throughout to denote the respective values in region I ($r<a$) and region II ($a<r<b$) (Fig. 1). In either region, the rf magnetic (electric) field of the fundamental TE (TM) mode has only a ϕ component (Fig. 1), which may be written in the general form as $[Aj(\xi)+By(\xi)]\sin\theta$. In this expression A and B are arbitrary constants, $\xi=kr$, where $k=\omega(\varepsilon\mu)^{1/2}$ is the wave number in the region whose (complex) permittivity and permeability are, respectively, ε and μ, and

$$j(\xi) = \frac{\sin\xi}{\xi^2} - \frac{\cos\xi}{\xi}, \tag{1}$$

$$y(\xi) = -\frac{\cos\xi}{\xi^2} - \frac{\sin\xi}{\xi} \tag{2}$$

are the spherical Bessel functions of order one. From these functions, we can construct the following functions:

$$J(\xi) = \xi j(\xi), \quad Y(\xi) = \xi y(\xi), \tag{3}$$

$$A(\xi) = \frac{J'(\xi)}{J(\xi)}, \quad B(\xi) = \frac{Y'(\xi)}{Y(\xi)}, \tag{4}$$

where, and hereafter, a prime denotes the derivative with respect to the argument. The dispersion relation for both the TE and TM modes and their damping rates are expressed in terms of these functions. The asymptotic formulas for these functions, as ξ approaches zero, are easily established:

$$j(\xi) \approx \xi/3, \quad y(\xi) \approx -1/\xi^2,$$

$$J(\xi) \approx \xi^2/3, \quad Y(\xi) \approx -1/\xi,$$

$$A(\xi) \approx 2/\xi, \quad B(\xi) \approx -1/\xi, \quad \xi \to 0. \tag{5}$$

These asymptotic expansions are needed to examine the limit of the empty cavity ($a=0$). We shall consider separately the TE mode and TM mode. With $e^{j\omega t}$ dependence, these modes satisfy the Maxwell equations, curl $\mathbf{E}=-j\omega\mu\mathbf{H}$ and curl $\mathbf{H}=j\omega\varepsilon\mathbf{E}$ in the respective regions I and II.

A. TE mode

The rf magnetic field of the TE_{110} mode has only a ϕ component, i.e., $\mathbf{H}=\hat{\phi}H_\phi$, where $\hat{\phi}$ is the unit vector in the ϕ direction. In region I, in order that the solutions are finite at $r=0$, we have

$$H_\phi = A(\sin\theta) j(k_1 r), \tag{6}$$

where A is an arbitrary constant and $k_1=\omega(\varepsilon_1\mu_1)^{1/2}$ is the wave number in region I. Use Eq. (6) in the Maxwell equation, $\mathbf{E}=\text{curl}\,\mathbf{H}/(j\omega\varepsilon_1)$, whose θ component yields

$$E_\theta = A(\sin\theta)\left(\frac{1}{j\omega\varepsilon_1 r}\right) J'(k_1 r). \tag{7}$$

In region II, H_ϕ is a linear combination of $j(k_2 r)$ and $y(k_2 r)$, where $k_2=\omega(\varepsilon_2\mu_2)^{1/2}$ is the wave number in region II. This linear combination must be chosen to render $E_\theta=0$ at $r=b$, the location of the perfectly conducting wall. This leads to

$$H_\phi = B(\sin\theta)[Y'(\eta) j(k_2 r) - J'(\eta) y(k_2 r)], \tag{8}$$

where B is an arbitrary constant and $\eta=k_2 b$. Analogous to Eq. (7), we then obtain

$$E_\theta = B(\sin\theta)\left(\frac{1}{j\omega\varepsilon_2 r}\right)[Y'(\eta) J'(k_2 r) - J'(\eta) Y'(k_2 r)], \tag{9}$$

which indeed satisfies $E_\theta=0$ at $r=b$.

The exact dispersion relation for the (complex) eigenmode frequency is obtained by demanding that the "admittance" matches at $r=a$. That is, the ratio H_ϕ/E_θ evaluated at $r=a$ using Eqs. (6) and (7) is the same as that using Eqs. (8) and (9). This condition is most conveniently written as

$$J'(\eta) = Y'(\eta)\left[\frac{J(\xi_2)}{Y(\xi_2)}\right]\left[\frac{Z_1 A(\xi_1) - A(\xi_2)}{Z_1 A(\xi_1) - B(\xi_2)}\right], \tag{10}$$

where, as defined in Eq. (8),

$$\eta = k_2 b = \omega b\sqrt{\varepsilon_2\mu_2}, \tag{11}$$

$$\xi_1 = k_1 a = \omega a\sqrt{\varepsilon_1\mu_1}, \quad \xi_2 = k_2 a = \omega a\sqrt{\varepsilon_2\mu_2}, \tag{12}$$

$$Z_1 = \frac{\sqrt{\mu_1/\mu_2}}{\sqrt{\varepsilon_1/\varepsilon_2}}. \tag{13}$$

Note from Eq. (13) that Z_1 is simply the ratio of the characteristic impedance $(\mu/\varepsilon)^{1/2}$ of the two regions, I and II. Equation (10) is the exact dispersion relation for the complex eigenfrequency (ω) of the TE_{110} mode, whose imaginary part is γ, the damping rate of the mode amplitude.

When the particulate is absent, the right-hand member of Eq. (10) vanishes. This can be seen in two ways. The first way is to let $\varepsilon_1=\varepsilon_2$ and $\mu_1=\mu_2$ so that region I and region II are the same medium. Then, $\xi_1=\xi_2$ and $Z_1=1$ from Eqs. (12) and (13), in which case the numerator in the second square bracket of Eq. (10) vanishes. The second way, which is more appropriate to the present paper, is to consider a vanishingly small particulate ($a=0$ limit). As a approaches zero, so does ξ_1 and ξ_2 according to Eq. (12). The asymptotic expansions listed in Eq. (5) may then be used at the right-hand member of Eq. (10) in this small a limit. It is immediately clear that the first square bracket in Eq. (10) vanishes like a^3, and that the second square bracket in Eq. (10) approaches a finite constant. Thus, the right-hand member of Eq. (10) is proportional to a^3 for a small particulate.

Thus, when the particulate is absent, the eigenfrequency of the TE_{110} mode ω_E is given by $J'(\eta_E)=0$, where

$$\eta_E = \omega_E b\sqrt{\varepsilon_2\mu_2} \equiv 2\pi b/\lambda = 2.743\,71 \tag{14}$$

is the first nontrivial root of $J'(\eta)$. In Eq. (14), $\lambda = 2\pi/[\omega_E(\varepsilon_2\mu_2)^{1/2}] = 2\pi b/\eta_E$ is the wavelength of an electromagnetic wave of frequency $\omega=\omega_E$ in a medium that is characterized by ε_2 and μ_2. Thus, specifying this frequency ω (or the wavelength λ) is the same as specifying b since η_E is a universal constant. The quasistatic limit $\omega=0$ is recovered by letting b (or λ) to become arbitrarily large.

The introduction of a small particulate modifies the eigenvalue η_E by a small amount, that is $\eta=\eta_E+\delta\eta$ and $\omega=\omega_E+\delta\omega$, where $\delta\omega/\omega_E=\delta\eta/\eta_E$ from the logarithmic derivative of Eq. (11). The left-hand member of Eq. (10), upon expanding about η_E, becomes $\delta\eta J''(\eta_E)$. We then immediately obtain from Eq. (10) the following explicit formulas on the particulate's modification of the eigenfrequency:

$$\frac{\delta\omega}{\omega_E} = \frac{\delta\eta}{\eta_E} \approx \frac{Y'(\eta_E)}{\eta_E J''(\eta_E)}\left[\frac{J(\xi_{2E})}{Y(\xi_{2E})}\right]\left[\frac{Z_1 A(\xi_{1E}) - A(\xi_{2E})}{Z_1 A(\xi_{1E}) - B(\xi_{2E})}\right], \tag{15}$$

$$\xi_{1E} = \omega_E a\sqrt{\varepsilon_1\mu_1} = 2\pi\left(\frac{a}{\lambda}\right)\sqrt{\frac{\varepsilon_1}{\varepsilon_2}\frac{\mu_1}{\mu_2}}, \tag{16}$$

$$\xi_{2E} = \omega_E a\sqrt{\varepsilon_2\mu_2} = 2\pi\left(\frac{a}{\lambda}\right). \tag{17}$$

The real part of Eq. (15) gives the detune of the eigenmode frequency and the imaginary part gives the damping rate, as a result of the particulate. We should stress that Eq. (15) is rather general. The only assumption that is made is that the particulate is small ($a/\lambda \ll 1$) so that its presence only introduces a small perturbation in the eigenfrequency of the TE_{110} mode under consideration. There is no restriction on the electrical conductivity of the particulate, nor is there any restriction on the frequency as long as $a/\lambda \ll 1$. Thus, the resistive skin depth associated with the particulate may assume an arbitrary value between zero and infinity, and Eq. (15) also covers the quasistatic limit.

At the right-hand member of Eq. (15), the only term that can contribute to an imaginary part is $Z_1A(\xi_{1E})$ since both η_E and ξ_{2E} are purely real. Since the damping rate γ_E of the TE_{110} mode may be obtained by extracting the imaginary part of Eq. (15), let us rewrite the second square bracket of Eq. (15) as $1+[B(\xi_{2E})-A(\xi_{2E})]/[Z_1A(\xi_{1E})-B(\xi_{2E})]$. The imaginary part of Eq. (15) then yields the normalized damping rate for the TE_{110} mode,

$$\frac{\gamma_E}{\omega_E} = \frac{Y'(\eta_E)}{\eta_E J''(\eta_E)}\frac{J(\xi_{2E})}{Y(\xi_{2E})}[B(\xi_{2E}) - A(\xi_{2E})] \times \mathrm{Im}\left[\frac{1}{Z_1A(\xi_{1E}) - B(\xi_{2E})}\right], \tag{18a}$$

which reduces to Eq. (1) of Ref. 17 for the special case of $\varepsilon_2=\varepsilon_0$ and $\mu_2=\mu_0$. Since $B(\xi_{2E})$ is real, we may divide both the numerator and denominator of Eq. (18a) by $B(\xi_{2E})$ to obtain

$$\frac{\gamma_E}{\omega_E} = \frac{Y'(\eta_E)}{\eta_E J''(\eta_E)}\left[\frac{J(\xi_{2E})}{Y(\xi_{2E})} - \frac{J'(\xi_{2E})}{Y'(\xi_{2E})}\right]\mathrm{Im}\left(\frac{1}{F-1}\right), \tag{18b}$$

$$F = \frac{Z_1A(\xi_{1E})}{B(\xi_{2E})} = \frac{\sqrt{\mu_1/\mu_2}}{\sqrt{\varepsilon_1/\varepsilon_2}}\frac{J'(\xi_{1E})}{J(\xi_{1E})}\frac{Y(\xi_{2E})}{Y'(\xi_{2E})}, \tag{18c}$$

where, according to Eq. (18b), the damping rate is dictated by F.

The damping rate (γ) of the eigenmode amplitude is related to the average power loss (P) and to the quality factor (Q) through the general relationship,[19,20]

$$P = 2\gamma U = \omega U/Q, \tag{19}$$

where U is the average electromagnetic energy stored in the eigenmode of the empty cavity whose natural frequency is ω. For the TE_{110} mode, this power may also be expressed in terms of the polarizability of the particulate α_E as[13,14,17]

$$P = \alpha_E\omega_E\left(\frac{1}{2}\varepsilon_2E_0^2\right)V_a \quad \text{(TE mode)}, \tag{20}$$

where E_0 is the peak value of the rf electric field of the TE mode at the center of the cavity in the absence of the particulate, whose volume is $V_a=(4\pi/3)a^3$. Comparing (19) and (20), we obtain

$$\alpha_E = 0.041\,31\left(\frac{\lambda}{a}\right)^3\frac{\gamma_E}{\omega_E}, \tag{21}$$

where (γ_E/ω_E) is given in Eq. (18a) or (18b). Equation (21) is derived in Appendix A [cf. Eq. (A7)].

B. TM Mode

The Ohmic dissipation in the particulate via the rf magnetic field may be similarly analyzed. Referring to Fig. 1(b), the rf electric field of the TM_{110} mode has only a ϕ component, i.e., $\mathbf{E}=\hat{\phi}E_\phi$, which in region I may be written as [cf. Eq. (6)]

$$E_\phi = C(\sin\theta)j(k_1r), \tag{22}$$

where C is an arbitrary constant. Taking the θ component of the Faraday's law, $\mathbf{H}=-\mathrm{curl}\,\mathbf{E}/(j\omega\mu_1)$, we obtain

$$H_\theta = C(\sin\theta)\left(\frac{1}{-j\omega\mu_1 r}\right)J'(k_1r). \tag{23}$$

In region II, in order that E_ϕ vanishes at $r=b$, it is of the form

$$E_\phi = D(\sin\theta)[y(\eta)j(k_2r) - j(\eta)y(k_2r)], \tag{24}$$

where D is an arbitrary constant and $\eta=k_2b$ as in Eq. (11). Analogous to Eq. (23), we then obtain

$$H_\theta = D(\sin\theta)\left(\frac{1}{-j\omega\mu_2 r}\right)[y(\eta)J'(k_2r) - j(\eta)Y'(k_2r)]. \tag{25}$$

The dispersion relation for the TM_{110} mode is obtained by requiring that the ratio E_ϕ/H_θ evaluated at $r=a$ using Eqs. (22) and (23) be the same as that using Eqs. (24) and (25). This condition is most conveniently written as

$$j(\eta) = y(\eta)\left[\frac{J'(\xi_2)}{Y'(\xi_2)}\right]\left[\frac{Z_1/A(\xi_1) - 1/A(\xi_2)}{Z_1/A(\xi_1) - 1/B(\xi_2)}\right], \tag{26}$$

where η, ξ_1, ξ_2, and Z_1 are the same as in Eqs. (11)–(13). Once more, when the particulate is absent, the right-hand member of Eq. (26) vanishes. More precisely, the right-hand member of Eq. (26) is proportional to a^3 as the particulate radius a tends to zero.

Thus, when the particulate is absent, the eigenfrequency of the TM_{110} mode ω_M is given by $j(\eta_M)=0$, where

$$\eta_M = \omega_M b\sqrt{\varepsilon_2\mu_2} \equiv 2\pi b/\lambda = 4.4934 \tag{27}$$

is the first nontrivial root of $j(\eta)$. In Eq. (27), $\lambda = 2\pi/[\omega_M(\varepsilon_2\mu_2)^{1/2}]=2\pi b/\eta_M$ is the wavelength of an electromagnetic wave of frequency $\omega=\omega_M$ in a medium that is characterized by ε_2 and μ_2, and η_M is a universal constant.

The introduction of a small particulate modifies the eigenvalue η_M and the eigenfrequency ω_M by a small amount. Analogous to Eq. (15), we obtain from Eq. (26) the modification of the eigenfrequency of the TM_{110} mode,

$$\frac{\delta\omega}{\omega_M} = \frac{\delta\eta}{\eta_M} \approx \frac{y(\eta_M)}{\eta_M j'(\eta_M)}\left[\frac{J'(\xi_{2M})}{Y'(\xi_{2M})}\right] \times\left[\frac{Z_1/A(\xi_{1M}) - 1/A(\xi_{2M})}{Z_1/A(\xi_{1M}) - 1/B(\xi_{2M})}\right], \tag{28}$$

$$\xi_{1M} = \omega_M a\sqrt{\varepsilon_1\mu_1} = 2\pi\left(\frac{a}{\lambda}\right)\sqrt{\frac{\varepsilon_1}{\varepsilon_2}\frac{\mu_1}{\mu_2}}, \tag{29}$$

$$\xi_{2M} = \omega_M a\sqrt{\varepsilon_2\mu_2} = 2\pi\left(\frac{a}{\lambda}\right). \tag{30}$$

Note that $\xi_{1M}=\xi_{1E}$ and $\xi_{2M}=\xi_{2E}$ for the same wavelength λ, by comparing Eq. (16) with Eq. (29), and Eq. (17) with Eq. (30). Analogous to Eq. (18a), the damping rate of the TM_{110} mode reads

$$\frac{\gamma_M}{\omega_M} = \frac{y(\eta_M)}{\eta_M j'(\eta_M)}\frac{J'(\xi_{2M})}{Y'(\xi_{2M})}\left[\frac{1}{B(\xi_{2M})} - \frac{1}{A(\xi_{2M})}\right] \times\mathrm{Im}\left[\frac{1}{Z_1/A(\xi_{1M}) - 1/B(\xi_{2M})}\right], \tag{31a}$$

which reduces to Eq. (3) of Ref. 17 for the special case of $\varepsilon_2=\varepsilon_0$ and $\mu_2=\mu_0$. Since $B(\xi_{2M})$ is real, we may multiply both the numerator and denominator of Eq. (31a) by $B(\xi_{2M})$ to obtain

$$\frac{\gamma_M}{\omega_M} = \frac{y(\eta_M)}{\eta_M j'(\eta_M)}\left[\frac{J'(\xi_{2M})}{Y'(\xi_{2M})} - \frac{J(\xi_{2M})}{Y(\xi_{2M})}\right]\mathrm{Im}\left(\frac{1}{G-1}\right), \tag{31b}$$

$$G = \frac{Z_1 B(\xi_{2M})}{A(\xi_{1M})} = \frac{\sqrt{\mu_1/\mu_2}}{\sqrt{\varepsilon_1/\varepsilon_2}}\frac{J(\xi_{1M})}{J'(\xi_{1M})}\frac{Y'(\xi_{2M})}{Y(\xi_{2M})}, \tag{31c}$$

where, according to Eq. (31b), the damping rate is dictated by G. Note the similarity between Eqs. (18b) and (31b).

The average power P absorbed by the particulate may be expressed in terms of the polarizability of the particulate α_H of the TM_{110} mode,[13,14,17]

$$P = \alpha_H\omega_M\left(\frac{1}{2}\mu_2 H_0^2\right)V_a \quad \text{(TM mode)}, \tag{32}$$

where H_0 is the peak value of the rf magnetic field of the TM mode at the center of the cavity in the absence of the particulate, whose volume is $V_a=(4\pi/3)a^3$. In Appendix A, we show that [cf. Eq. (A13)]

$$\alpha_H = 0.077\,67\left(\frac{\lambda}{a}\right)^3\frac{\gamma_M}{\omega_M}, \tag{33}$$

where (γ_M/ω_M) is given in Eq. (31a) or (31b).

III. NUMERICAL RESULTS AND SCALING FORMULAS

In Sec. II, we derive the polarizabilities, α_E and α_H, which, respectively, measures the degree of absorption in a particulate that is exposed to a pure TE mode and to a pure TM mode. In the absence of the particulate, the medium is characterized by the permittivity and permeability ε_2 and μ_2, both assumed real. The particulate's permeability μ_1 is also assumed real, while its permittivity $\varepsilon_1=\varepsilon_{1r}+\sigma/j\omega$ is in general complex, where σ is the particulate's electrical resistivity. Since the wavelength and the energy density that appear in Eqs. (20) and (32) refer to region II, we express the particulate's parameters in terms of the quantities in region II. Thus, we write

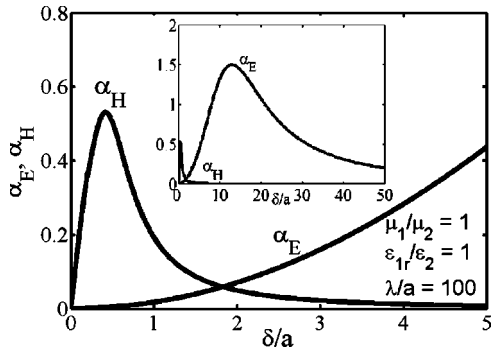

FIG. 2. The polarizabilities α_E and α_H as a function of δ/a for $\mu_1/\mu_2=1$, $\varepsilon_{1r}/\varepsilon_2=1$, and $\lambda/a=100$.

$$\frac{\varepsilon_1}{\varepsilon_2} = \frac{\varepsilon_{1r}}{\varepsilon_2}\left(1 - j\frac{\sigma}{\omega\varepsilon_{1r}}\right) = \frac{\varepsilon_{1r}}{\varepsilon_2}\left[1 - j\frac{1}{2\pi^2}\left(\frac{\lambda}{\delta}\right)^2\left(\frac{\varepsilon_2}{\varepsilon_{1r}}\right)\right], \tag{34}$$

$$\delta = \sqrt{\frac{2}{\omega\mu_2\sigma}}, \tag{35}$$

where $\lambda=2\pi/[\omega(\varepsilon_2\mu_2)^{1/2}]$ is the wavelength in region II and δ is the resistive skin depth defined with respect to μ_2, the permeability of region II.

The polarizabilities α_E and α_H depend on four dimensionless parameters: δ/a, a/λ, $\varepsilon_{1r}/\varepsilon_2$, and μ_1/μ_2. To see this, the product of the first two yields δ/λ, and Eq. (34) then shows that $\varepsilon_1/\varepsilon_2$ may be expressed in terms of these four parameters. It immediately follows that ξ_{1E} and ξ_{2E}, and therefore γ_E/ω_E and α_E, are functions of these four dimensionless parameters according to Eqs. (16)–(18). A similar argument applies to α_H.

Figure 2 shows α_E and α_H as a function of δ/a, setting $\mu_1/\mu_2=1$, $\varepsilon_{1r}/\varepsilon_2=1$, and $\lambda/a=100$. These curves are obtained from Eqs. (21) and (33). It can be seen from Fig. 2 that the polarizability for the TM mode (α_H) dominates for small δ/a. For large δ/a, the polarizability for the TE mode (α_E) surpasses that of the TM mode. The inset of Fig. 2 shows α_E and α_H on a much larger scale. Since the polarizability is directly proportional to the power absorbed, for small δ/a the power absorbed by the particulate when it is exposed to an electromagnetic wave is, in general, primarily through the rf magnetic field, whereas for large δ/a, the power absorbed is primarily through the rf electric field. For very large δ/a, both α_E and α_H tend to zero, as expected of an almost nonconducting particulate.

Figure 3 shows α_H for different ratios of λ/a with $\mu_1/\mu_2=1$ and $\varepsilon_{1r}/\varepsilon_2=1$. The insensitivity of α_H to λ/a, for large values of λ/a, is apparent in Fig. 3. Also superimposed in Fig. 3 are the approximations according to asymptotic formulas for α_H,

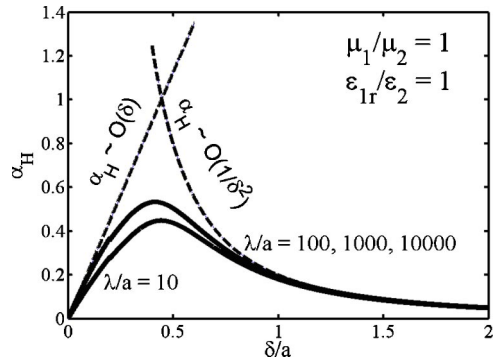

FIG. 3. The polarizability α_H as a function of δ/a for $\mu_1/\mu_2=1$, $\varepsilon_{1r}/\varepsilon_2=1$, and various values of λ/a. The dotted curves show the asymptotic formulas.

$$\alpha_H \cong \frac{9}{4}\left(\frac{\delta}{a}\right)\sqrt{\frac{\mu_1}{\mu_2}}, \quad \sqrt{\frac{\mu_2}{\mu_1}}\frac{\delta}{a} \ll 1, \tag{36a}$$

$$\alpha_H \cong \frac{1}{5}\left(\frac{a}{\delta}\right)^2\left(\frac{\mu_1}{\mu_2}\right)^2\left(\frac{3}{2+\mu_1/\mu_2}\right)^2, \quad \sqrt{\frac{\mu_2}{\mu_1}}\frac{\delta}{a} \gg 1. \tag{36b}$$

We shall also record the asymptotic formulas for α_E,

$$\alpha_E \cong 9\pi^2\left(\frac{a\delta}{\lambda^2}\right)\sqrt{\frac{\mu_1}{\mu_2}}, \quad \sqrt{\frac{\mu_2}{\mu_1}}\frac{\delta}{a} \ll 1; \tag{37a}$$

$$\alpha_E \cong 18\pi^2(\delta/\lambda)^2, \quad 1 \ll \sqrt{\frac{\mu_2}{\mu_1}}\frac{\delta}{a} \ll \frac{1}{\pi\sqrt{2}}\sqrt{\frac{\varepsilon_2}{\varepsilon_{1r}}}\sqrt{\frac{\mu_2}{\mu_1}}\left(\frac{\lambda}{a}\right); \tag{37b}$$

$$\alpha_E \cong \frac{(\lambda/\delta)^2}{2\pi^2}\left(\frac{3}{2+\varepsilon_{1r}/\varepsilon_2}\right)^2, \quad 1 \ll \frac{1}{\pi\sqrt{2}}\sqrt{\frac{\varepsilon_2}{\varepsilon_{1r}}}\sqrt{\frac{\mu_2}{\mu_1}}\left(\frac{\lambda}{a}\right) \ll \sqrt{\frac{\mu_2}{\mu_1}}\frac{\delta}{a}. \tag{37c}$$

The asymptotic expansions for α_H, Eqs. (36), are obtained by using the appropriate asymptotic expansions of Eq. (31b) into Eq. (33). The asymptotic expansions for α_E, Eqs. (37), are obtained by using the appropriate asymptotic expansions of Eq. (18b) into Eq. (21). The scalings given in Eqs. (36) and (37) are applicable to general values of ε_2 and μ_2 in region II. They are generalizations of Ref. 17, which focused only on the special case $\mu_1=\mu_2=\mu_0$ and $\varepsilon_{1r}=\varepsilon_2=\varepsilon_0$. A simplified derivation of (36) and (37), based on physical arguments aided by a dimensional analysis, is given in Appendix B.

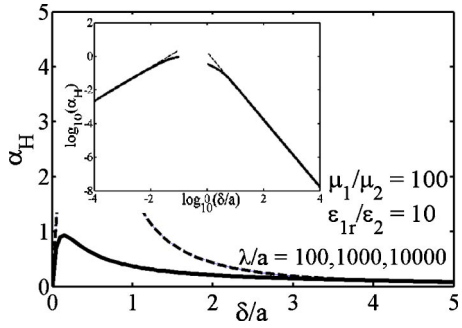

FIG. 5. The polarizability α_H as a function of δ/a for $\mu_1/\mu_2=100$, $\varepsilon_{1r}/\varepsilon_2=10$, and various values of λ/a. The dotted curves show the asymptotic formulas. The inset shows an expanded range of δ/a.

Figure 4 shows α_E for different ratios of λ/a with $\mu_1/\mu_2=1$ and $\varepsilon_{1r}/\varepsilon_2=1$. Also shown in Fig. 4 are the asymptotic expansions, in which $\delta/a \sim O(1)$ marks the transition from Eq. (37a) to Eq. (37b); whereas the maxima of α_E, which occur approximately when $\sigma=\omega\varepsilon_{1r}$, mark the transition from Eq. (37b) and (37c).

In Figs. 5 and 6, we show, respectively, α_H and α_E for different ratios of λ/a with $\mu_1/\mu_2=100$ and $\varepsilon_{1r}/\varepsilon_2=10$. The asymptotic expansions, Eqs. (36) and (37), are also shown in these figures. These two figures demonstrate the applicability of the theory to arbitrary values of μ_1, μ_2, ε_{1r}, and ε_2, and over a total of 12 orders of magnitude among δ, a, and λ. Once more, α_H dominates over α_E when $\delta/a \ll 1$ by examining the scales in Figs. 5 and 6, thus perhaps offering a plausible explanation for the results of Refs. 2 and 9.

IV. HEATING OF PARTICULATE BY A FINITE PULSE

In this section, we use the results obtained in the preceding sections to assess the total energy absorbed by a particulate when it is exposed to a transient electric field (or transient magnetic field) of a finite pulse duration. Several assumptions are made. First, it is assumed that $a \ll \lambda$ for all frequency contents in that finite pulse. Second, we assume

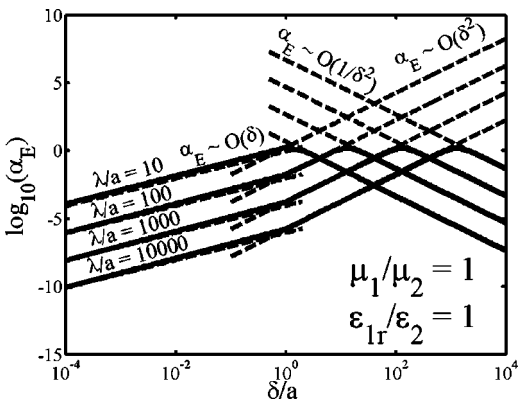

FIG. 4. The polarizability α_E as a function of δ/a for $\mu_1/\mu_2=1$, $\varepsilon_{1r}/\varepsilon_2=1$, and various values of λ/a. The dotted curves show the asymptotic formulas.

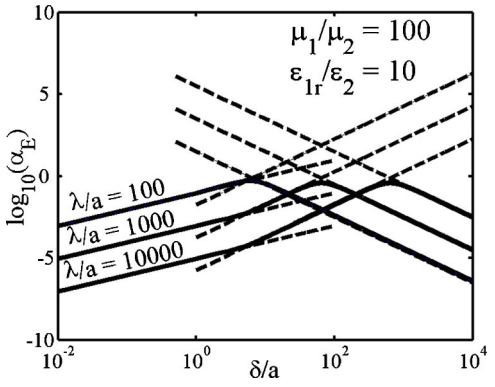

FIG. 6. The polarizability α_E as a function of δ/a for $\mu_1/\mu_2=100$, $\varepsilon_{1r}/\varepsilon_2=10$, and various values of λ/a. The dotted curves show the asymptotic formulas.

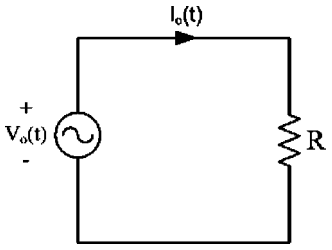

FIG. 7. A circuit model for Ohmic heating of a particulate by a rf electric field.

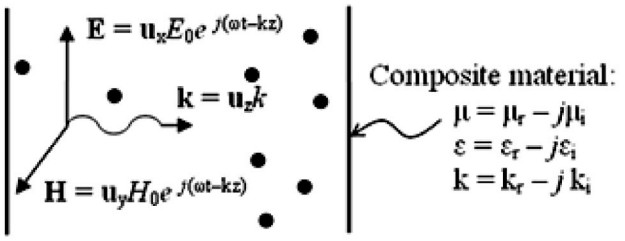

FIG. 8. Composite material, consisting of a lossless dielectric seeded with spherical particulates.

that the frequency dependence in $\varepsilon_{1r}(\omega)$, $\mu_1(\omega)$, and $\sigma(\omega)$ is known in the frequency band that makes up the finite pulse.

Let us first consider a finite electric pulse. We shall use a circuit model (Fig. 7), where the particulate is modeled as a lump resistor (R) and the external electric field (E_0) is modeled as a voltage source (V_0). For scaling purposes, we assume that $V_0=E_0D$ for some arbitrary constant D. When the external electric field is in a sinusoidal steady state of frequency ω, $E_0(t)=E(\omega)e^{j\omega t}$, the average power deposited into the particulate is [cf. Eq. (20)]

$$P = \alpha_E \omega_E \left[\frac{1}{2}\varepsilon(\omega)^2\right] V_a. \tag{38}$$

Since this average power must be the same as that dissipated in the lumped resistance, $V^2/2R=D^2E^2(\omega)/2R$, and we obtain

$$R(\omega) = \frac{V(\omega)}{I(\omega)} = \frac{D^2}{\varepsilon_2 \omega \alpha_E(\omega) V_a}. \tag{39}$$

A finite pulse of the electric field $E_0(t)$ may be represented in terms of its Fourier transform $E(\omega)$,

$$E_0(t) = \int d\omega E(\omega) e^{j\omega t}, \tag{40}$$

with a corresponding voltage $V_0(t)=E_0(t)D$, and the associated Fourier transform $V(\omega)=E(\omega)D$. The total energy W_E dissipated in the particulate during this finite electric-field pulse is then given by (Fig. 7)

$$W_E = \int dt V_0(t) I_0(t) = \frac{1}{2}\,\mathrm{Re}\int d\omega V(\omega) I^*(\omega)$$

$$= \int d\omega \alpha_E(\omega) \frac{1}{2}\omega\varepsilon_2 |E(\omega)|^2 V_a, \tag{41}$$

where $I_0(t)$ is the current flowing through the resistor, and we have used the Parseval's theorem and Eq. (39). The analytic expressions given in Eq. (37) for α_E allow a ready assessment of W_E once the Fourier spectrum of the electric-field pulse $|E(\omega)|^2$ is given.

Similarly, when this particulate is exposed to an external magnetic field of a finite pulse length, the total energy W_M absorbed by the particulate is given by

$$W_M = \int d\omega \alpha_H(\omega) \frac{1}{2}\omega\mu_2 |H(\omega)|^2 V_a, \tag{42}$$

where $|H(\omega)|^2$ is the Fourier spectrum of the external magnetic-field pulse. Again, the asymptotic formula for α_H, Eq. (36), provides a convenient estimate of this magnetic energy dissipation. When the particulate is exposed to a transient electromagnetic pulse, the total energy absorbed is the sum of Eqs. (41) and (42).

V. POWER LOSSES IN A COMPOSITE DIELECTRIC

The analysis of power absorption in a single particulate, described in the previous sections of this paper, may be extended to study the attenuation of electromagnetic waves due to a collection of particulates in a composite dielectric. The composite material is assumed to consist of a lossless dielectric, randomly and sparsely seeded with identical spherical particulates, as shown in Fig. 8. The number density of the sphere n is assumed to be low enough that adjacent spheres do not interact with each other. This assumption is reasonable at low number densities, since the interaction between different spheres is primarily through dipole fields which decrease in magnitude as $1/r^3$. Thus, this assumption is essentially $a \ll \ell$, where a is the particulate radius and $\ell = n^{-1/3}$ is the average interparticulate separation.

The composite material has an effective macroscopic permittivity $\varepsilon=\varepsilon_r-j\varepsilon_i$ and macroscopic permeability $\mu=\mu_r-j\mu_i$. The imaginary parts of ε and μ are due to the power-absorbing particulates embedded in the material and are assumed to be small due to the low number density of particulates. The wave number $k=\omega\sqrt{\mu\varepsilon}=k_r-jk_i$ will therefore have a small imaginary part k_i given by

$$k_i \cong \frac{1}{2}\omega\sqrt{\mu_2\varepsilon_2}\left(\frac{\mu_i}{\mu_2}+\frac{\varepsilon_i}{\varepsilon_2}\right), \tag{43}$$

and a real part $k_r \cong \omega\sqrt{\mu_2\varepsilon_2}$, where μ_2 and ε_2 are, respectively, the permeability and permittivity of the dielectric void of particulates. The time-averaged Poynting flux is given by $\mathbf{S}=\frac{1}{2}\,\mathrm{Re}(\mathbf{E}\times\mathbf{H}^*)$. For a plane wave traveling in the z direction, the Poynting flux is therefore

$$\mathbf{S} = \hat{z} S_0 e^{-2k_i z}, \tag{44}$$

with $S_0=E_0^2/2\eta=\eta H_0^2/2$ and $\eta \cong \sqrt{\mu_2/\varepsilon_2}$.

The Poynting flux in the z direction may also be obtained from a power balance over an incremental volume element $A\Delta z$,

$$S(z)A - S(z+\Delta z)A = (nA\Delta z)P, \tag{45}$$

in terms of the Poynting flux S, the number density n of the particulates in the composite material, and the power P absorbed by a single particulate. We divide Eq. (45) by $A\Delta z$ and take the limit as $\Delta z \to 0$ to obtain

$$-\frac{dS}{dz} = n\alpha_E \omega \left(\frac{1}{2}\varepsilon_2 E^2\right) V_a, \tag{46a}$$

$$-\frac{dS}{dz} = n\alpha_H \omega \left(\frac{1}{2}\mu_2 H^2\right) V_a. \tag{46b}$$

In Eq. (46a), the power absorbed by a single particulate, P in Eq. (45), is replaced with the expression in Eq. (20) for the case of purely rf electric-field losses, while in Eq. (46b) the expression in Eq. (32) is used for the case of purely rf magnetic-field losses. On the right-hand side of Eqs. (46a) and (46b) we may substitute for the Poynting flux, $S = \sqrt{\varepsilon_2/\mu_2}E^2/2 = \sqrt{\mu_2/\varepsilon_2}H^2/2$, and integrate the expressions to obtain

$$S = S_0 \exp(-n\alpha_E \omega \sqrt{\mu_2 \varepsilon_2} V_a z), \tag{47a}$$

$$S = S_0 \exp(-n\alpha_H \omega \sqrt{\mu_2 \varepsilon_2} V_a z), \tag{47b}$$

for, respectively, purely rf electric-field losses and purely rf magnetic-field losses.

A comparison of Eqs. (43), (44), and (47) yields the following expressions for the imaginary parts of the permittivity and permeability of the composite material:

$$\frac{\varepsilon_i}{\varepsilon_2} = \frac{4\pi}{3}\alpha_E \left(\frac{a}{\ell}\right)^3, \tag{48a}$$

$$\frac{\mu_i}{\mu_2} = \frac{4\pi}{3}\alpha_H \left(\frac{a}{\ell}\right)^3. \tag{48b}$$

In deriving Eq. (48a), the power losses were assumed to be purely due to rf electric-field interactions, where μ_i was neglected. Similarly, in Eq. (48b), the power losses were assumed to be due to rf magnetic-field interactions, where ε_i was neglected. Equation (43) shows that the spatial attenuation rate is the sum of these two contributions. If we define the equivalent "loss tangent" in the composite dielectric in terms of the total attenuation rate, we substitute Eqs. (48a) and (48b) into Eq. (43) to obtain

$$\tan \delta_{\text{loss}} = \frac{\mu_i}{\mu_2} + \frac{\varepsilon_i}{\varepsilon_2} = \frac{4\pi}{3}\left(\frac{a}{\ell}\right)^3 (\alpha_E + \alpha_H), \tag{49}$$

which is the equivalent loss tangent of the composite dielectric.

As a final note, the expressions for α_E and α_H are known over almost the entire frequency spectrum [up to $a \ll \lambda$; cf. Eqs. (21) and (33)]. The real parts of ε and μ can therefore be approximately calculated from Eqs. (48a) and (48b), respectively, by means of the Kramers–Kronig relationship.[21]

VI. REMARKS

In this paper, we have presented a rather complete theory on the heating of a homogeneous, spherical particulate by an electromagnetic field whose wavelength λ is long compared with the particulate radius a. By considering the local electromagnetic field as a linear combination of a TE mode and a TM mode, the Ohmic dissipation on each component may be evaluated from the polarizabilities α_E and α_H. Explicit expressions for these dimensionless quantities, together with their simple asymptotic forms, are derived. The energy delivered to the particulate from a finite electromagnetic pulse of general spectrum may be evaluated immediately, bypassing the difficult calculation of the temporal-spatial distribution of the electromagnetic field within the particulate. The only input required is ε_1 and μ_1 over the frequency band that makes up the pulse, and these quantities are presumably obtained from empirical data. The loss tangent is also constructed for a dielectric slab that is embedded from a sparsely populated distribution of such particulates. The formulation is valid from the static case to high frequency, regardless of the value of the resistive skin depth, as long as $a \ll \lambda$. The particulates may be located in a general lossless medium characterized by ε_2 and μ_2, and the theory is applicable over a wide range of parameters, as shown in Figs. 5 and 6.

The highly symmetrical model given in Sec. II may be extended to the case of a long, thin "particulate." One may simply model this as a long cylinder and place it at the center axis of a cylindrical waveguide. The power dissipated per unit axial length for the TE and TM modes may then be similarly constructed from the attenuation rate in such a highly symmetrical geometry. A simple argument shows that there will be a marked difference, depending on the polarization of the electric field (the limiting cases being the E field parallel to and orthogonal to the axis of the cylinder, with the most general case somewhere in between). Simple scaling laws may be similarly constructed.

The strictly spherical geometry shown in Figs. 1(a) and 1(b) may be analyzed for the higher-order TE and TM modes, as well as the perturbations on these modes due to the particulate. It is expected that many features of the Mie scattering by a lossy spherical particulate may be revealed from this highly symmetrical model.

In this paper we have concentrated only on the dissipative characteristics introduced by the particulates. The modifications in the reactive characteristics were largely ignored. While the corrections to the real part of the eigenfrequency, as given by Eqs. (15) and (28), respectively, for the TE and TM modes, would give some indication on the reactive loading due to the particulate, it is unclear how a collection of particulates would affect the real part of the dielectric function in a composite dielectric, such as the one shown in Fig. 8. On the other hand, it is interesting to ponder if this real part of the dielectric function could be computed from the imaginary part using the Krammer–Kronig relation. The imaginary part is given by Eq. (48a) in which α_E is computed over the wide range of frequencies, as given in Secs. II and III of this paper. Similar comments apply to the calculation on the real part of the permeability from its imaginary part, Eq. (48b).

Finally, the analytic expressions for the complex eigenfrequencies, Eqs. (15) and (28), may be used as a benchmark for advanced eigenmode solvers under the most stringent conditions.

ACKNOWLEDGMENTS

We thank Bahman Hafizi, John Luginsland, David Chernin, Arne Fliflet, John Booske, and Jeff Calame for useful discussions on various aspects of this problem. This work was supported by DOE Grant No. DE-FG02-98ER54475, AFOSR, DUSD (S & T) under the Innovative Microwave Vacuum Electronics MURI Program, managed by the Air Force Office of Scientific Research under Grant No. F49620-99-1-0297. It was also funded through AFOSR by a USDoD MURI04 grant on Cathodes and RF Windows.

APPENDIX A: DERIVATION OF EQS. (21) AND (33)

To derive α_E, we first equate Eqs. (19) and (20) to yield

$$\alpha_E = C_E(\gamma_E/\omega_E), \tag{A1}$$

$$C_E = \frac{4U}{\varepsilon_2 E_0^2 V_a}, \tag{A2}$$

where U is the total averaged energy stored in the TE_{110} mode of the unperturbed cavity (i.e., cavity in the absence of the particulate), E_0 is the peak value of the rf electric field at the center of the unperturbed cavity, and $V_a=(4\pi/3)a^3$ is the volume of the particulate. For any resonant-cavity mode, the averaged energy stored in the rf electric field is the same as that stored in the rf magnetic field. That is, U is twice the averaged energy stored in the rf magnetic field. Thus we write, in spherical coordinates,

$$U = 2\int d\nu\left(\frac{1}{4}\mu_2|\mathbf{H}|^2\right) = 2\int_0^b dr\int_0^{2\pi} rd\phi\int_0^{\pi} r\sin\theta d\theta\left(\frac{1}{4}\mu_2|H_\phi|^2\right), \tag{A3}$$

where we have used the fact that $\mathbf{H}$ has only the ϕ component for the TE_{110} mode [Fig. 1(a)].

For the unperturbed TE_{110} mode, the rf field solutions, Eqs. (6) and (7) apply for all $r<b$, provided k_1 and ε_1 in these two equations are to be replaced, respectively, by $k_2=\omega(\varepsilon_2\mu_2)^{1/2}$ and ε_2. With this replacement in Eq. (6), and then substituting Eq. (6) into Eq. (A3), we obtain

$$U = \mu_2|A|^2\left(\frac{4\pi}{3}b^3\right)\frac{g(\eta_E)}{\eta_E^3}, \tag{A4}$$

$$g(x) = \int_0^x d\xi\xi^2 j^2(\xi), \tag{A5}$$

where $\eta_E=k_2b=2.743\,71$ is the same as in Eq. (14) and $j(\xi)$ is defined in Eq. (1). To obtain Eq. (A4), we have also used the formula

$$\int_0^{\pi} d\theta\sin^3\theta = \frac{4}{3}.$$

The peak value of the rf electric field E_0 of the unperturbed TE_{110} mode occurs at the center of the cavity [Fig. 1(a)]. It is most easily obtained from Eq. (7) by evaluating its right-hand member at $\theta=\pi/2$, and by taking the limit $r=0$, with the understanding that k_1 and ε_1 in Eq. (7) are to be replaced, respectively, by $k_2=\omega(\varepsilon_2\mu_2)^{1/2}$ and ε_2, as explained above. Upon applying the asymptotic formula, $J'(\xi)\sim 2\xi/3$ as ξ tends to zero [cf. Eq. (5)], we obtain from Eq. (7)

$$E_0 = |E_\theta(r\to 0,\theta=\pi/2)| = \frac{2|A|}{3}\sqrt{\frac{\mu_2}{\varepsilon_2}}. \tag{A6}$$

Substituting Eqs. (A6) and (A4) into Eq. (A2), we obtain C_E. Equation (A1) then reads

$$\alpha_E = 9\left(\frac{\lambda}{2\pi a}\right)^3 g(\eta_E)\left(\frac{\gamma_E}{\omega_E}\right) = 0.041\,31\left(\frac{\lambda}{a}\right)^3\left(\frac{\gamma_E}{\omega_E}\right), \tag{A7}$$

where we have used the numerical value of $g(\eta_E)=1.1385$ and the definition of the wavelength λ according to Eq. (14) for the TE_{110} mode. Equation (A7) is the same as Eq. (21) of the main text.

To derive α_H, we use the entirely analogous approach by first equating Eqs. (19) and (32) to yield

$$\alpha_H = C_M(\gamma_M/\omega_M), \tag{A8}$$

$$C_M = \frac{4U}{\mu_2 H_0^2 V_a}, \tag{A9}$$

where U is the total averaged energy stored in the TM_{110} mode of the unperturbed cavity (i.e., cavity in the absence of the particulate), H_0 is the peak value of the rf magnetic field at the center of the unperturbed cavity, and $V_a=(4\pi/3)a^3$. Once more, the averaged energy stored in the rf electric field is the same as that stored in the rf magnetic field. That is, U is twice the averaged energy stored in the rf electric field. Thus we write, in spherical coordinates,

$$U = 2\int d\nu\left(\frac{1}{4}\varepsilon_2|\mathbf{E}|^2\right) = 2\int_0^b dr\int_0^{2\pi} rd\phi\int_0^{\pi} r\sin\theta d\theta\left(\frac{1}{4}\varepsilon_2|E_\phi|^2\right), \tag{A10}$$

where we have used the fact that $\mathbf{E}$ has only the ϕ component for the TM_{110} mode [Fig. 1(b)].

For the unperturbed TM_{110} mode, the rf field solutions, Eqs. (22) and (23) apply for all $r<b$, provided k_1 and μ_1 in these two equations are to be replaced, respectively, by $k_2=\omega(\varepsilon_2\mu_2)^{1/2}$ and μ_2. With this replacement, substitution of Eq. (22) into Eq. (A10) yields

$$U = \varepsilon_2|C|^2\left(\frac{4\pi}{3}b^3\right)\frac{g(\eta_M)}{\eta_M^3}, \tag{A11}$$

where the function g is defined in Eq. (A5) and η_M in Eq. (27).

Similarly, the peak value of the rf magnetic field H_0 of the unperturbed TM_{110} mode occurs at the center of the cavity and may be written as

$$H_0 = |H_\theta(r\to 0,\theta=\pi/2)| = \frac{2|C|}{3}\sqrt{\frac{\varepsilon_2}{\mu_2}}, \tag{A12}$$

where we have used Eq. (23). Substituting Eqs. (A11) and (A12) into Eq. (A9), we obtain C_M. Equation (A8) then reads

$$\alpha_H = 9\left(\frac{\lambda}{2\pi a}\right)^3 g(\eta_M)\left(\frac{\gamma_M}{\omega_M}\right) = 0.077\,67\left(\frac{\lambda}{a}\right)^3\left(\frac{\gamma_M}{\omega_M}\right), \tag{A13}$$

where we have used the numerical value of $g(\eta_M)=2.1407$ and the definition of the wavelength λ according to Eq. (27) for the TM_{110} mode. Equation (A13) is the same as Eq. (33) of the main text. Note the similarity between Eqs. (A7) and (A13).

APPENDIX B: DERIVATION OF EQS. (36) AND (37)

This appendix presents a simple derivation of Eqs. (36) and (37). For simplicity, in this Appendix, we consider only the special case $\mu_1=\mu_2=\mu_0$ and $\varepsilon_2=\varepsilon_0$. The exact scaling, including the numerical coefficients, can easily be found in the large skin depth regime ($\delta \gg a$) for both TE and TM cases. Similar calculations in the small skin depth regime ($\delta \ll a$) are, however, much more intricate, and hence we will present only "bare bone" derivation in the latter regime to obtain the appropriate parameter scaling.

1. TM mode, small skin depth regime ($\delta \ll a$)

For a nonmagnetic material, where $\mu=\mu_0$, the electric and magnetic fields inside the sphere are governed by

$$\nabla \times \mathbf{E}_1 = -\mu_0\frac{\partial \mathbf{H}_1}{\partial t} = -j\omega\mu_0\mathbf{H}_1. \tag{B1}$$

The fields, however, only penetrate a few skin depths into the sphere, so that we anticipate qualitatively that

$$\frac{E_I}{\delta} \sim \omega\mu_0 H_I, \tag{B2}$$

where $H_I=|\mathbf{H}_1(r=a)|$ and $E_I=|\mathbf{E}_1(r=a)|$.

The continuity of normal B and tangential H at $r=a$ leads to $H_I(r=a)=H_0$. The volume over which power is absorbed in the sphere can be approximated as a thin spherical shell of radius a and thickness δ. By neglecting the constant coefficients, the absorbed power scales as

$$P = \frac{1}{2}\int dV\sigma|\mathbf{E}_1|^2 \sim (4\pi a^2\delta)\sigma(\delta\omega\mu_0 H_0)^2. \tag{B3}$$

By substituting $(\sigma/\omega\varepsilon_0)=(1/2\pi^2)(\lambda/\delta)^2$ and neglecting the constant coefficients, we find

$$P \sim \frac{\delta}{a}\omega\left(\frac{1}{2}\mu_0 H_0^2\right)V_a. \tag{B4}$$

The scaling for the magnetic polarizability in the small skin depth regime, as given by Eq. (36a) except for the constant coefficient, is therefore

$$\alpha_H \sim \frac{\delta}{a}. \tag{B5}$$

2. TM mode, large skin depth regime ($\delta \gg a$)

In the large skin depth regime for a nonmagnetic material, where $\mu=\mu_0$, the continuity of normal B and tangential H demand that $\mathbf{H}_1=\hat{z}H_1=\hat{z}H_0$. The integral form of Faraday's equation is given by

$$\oint \mathbf{E}_1\cdot d\ell = -\mu_0\int_S \frac{\partial \mathbf{H}_1}{\partial t}\cdot d\mathbf{S}, \tag{B6}$$

where the electric field is of the form $\mathbf{E}_1=\hat{\phi}E_I$. Solving the integral equation in cylindrical coordinates gives $E_I 2\pi R = -j\omega\mu_0 H_0\pi R^2$. By canceling out terms and converting from cylindrical to spherical coordinates by substituting $R=r\sin\theta$ (see Fig. 1), we obtain

$$\mathbf{E}_1 = -\hat{\phi}j\omega\mu_0\frac{H_0}{2}r\sin\theta. \tag{B7}$$

The power absorbed in the sphere is given by

$$P = \frac{1}{2}\int \sigma|\mathbf{E}_1|^2 dV = \frac{\sigma\omega^2\mu_0^2H_0^2}{8}\int_0^{2\pi}d\phi\int_0^{\pi}\sin^3\theta d\theta\int_0^a r^4 dr,$$

$$P = \frac{1}{5}\left(\frac{a}{\delta}\right)^2\omega\left(\frac{1}{2}\mu_0 H_0^2\right)V_a. \tag{B8}$$

The magnetic polarizability in the large skin depth regime, shown in Eq. (36b), is therefore given by

$$\alpha_H = \frac{1}{5}\left(\frac{a}{\delta}\right)^2. \tag{B9}$$

3. TE mode, small skin depth regime ($\delta \ll a$)

With the assumption that $\sigma \gg \omega\varepsilon_{1r}$, we may neglect the displacement current in Ampére's equation to write $\nabla\times\mathbf{H}_1 \cong \sigma\mathbf{E}_1$. The fields only penetrate a few skin depths into the sphere, which allows us to approximate this equation as

$$\frac{H_I}{\delta} \cong \sigma E_I, \tag{B10}$$

where $\mathbf{H}_1=\hat{\phi}H_I$ [Fig. 1(a)].

The continuity of tangential H at $r=a$ demands that $H_I(r=a)=H_{II}(r=a)$. The field solution for H_ϕ in region II is approximately given by Eq. (6), in which k_1 is replaced by $k_2=\omega(\varepsilon_0\mu_0)^{1/2}$. Since the argument of the Bessel function $j(k_2 r)$ at $r\sim a$ may be considered "small" for $a \ll b$, the field solution at $r\sim a$ will, to the lowest order, scale linearly in r [cf. Eq. (5)]. This allows us to write the external magnetic field, with $k_2=2\pi/\lambda$, as

$$H_{II}(r=a) \sim (\text{const})\times(a/\lambda)H_0, \tag{B11}$$

where H_0 is the maximum value of the rf magnetic field in region II [Fig. 1(a)]. Neglecting the constants, we may now write the expression for the electric field inside the sphere as

$$E_I \sim \frac{1}{\sigma\delta}\left(\frac{a}{\lambda}\right)H_0. \tag{B12}$$

The volume over which power is absorbed in the sphere can be approximated as a thin spherical shell of radius a and thickness δ. By again neglecting the constant coefficients, the absorbed power scales as

$$P = \frac{1}{2}\int dV\sigma|\mathbf{E}_1|^2 \sim (4\pi a^2\delta)\sigma\frac{1}{\sigma^2\delta^2}\left(\frac{a}{\lambda}\right)^2 H_0^2. \tag{B13}$$

By substituting $(\sigma/\omega\varepsilon_0)=(1/2\pi^2)(\lambda/\delta)^2$ and noting that $\varepsilon_0 E_0^2 \sim \mu_0 H_0^2$, where E_0 and H_0 is, respectively, the maximum rf electric and maximum rf magnetic field of the unperturbed TE_{110} mode, we find

$$P \sim \frac{a\delta}{\lambda^2}\omega\left(\frac{1}{2}\varepsilon_0 E_0^2\right)V_a. \tag{B14}$$

The scaling for α_E in the thin skin depth regime as shown in Eq. (37a) is therefore recovered (except for the constant coefficient),

$$\alpha_E \sim \frac{a\delta}{\lambda^2}. \tag{B15}$$

4. TE mode, large skin depth regime $(\delta \gg a)$

The asymptotic formulas in the large skin depth regime can be obtained by considering a sphere exposed to a uniform rf electric field [Fig. 1(a)]. Outside the sphere, the imposed field is

$$\mathbf{E}_0(\mathbf{r},t) = \hat{z}E_0 e^{j\omega t} = (\hat{r}\cos\theta - \hat{\theta}\sin\theta)E_0 e^{j\omega t}. \tag{B16}$$

The sphere also sets up a dipole field outside of the sphere, described by

$$\mathbf{E}_d(\mathbf{r},t) = E_d\left(\frac{a}{r}\right)^3(\hat{r}2\cos\theta + \hat{\theta}\sin\theta)e^{j\omega t}. \tag{B17}$$

Inside the sphere, the E field is uniform,

$$\mathbf{E}_1(\mathbf{r},t) = \hat{z}E_1 e^{j\omega t} = E_1(\hat{r}\cos\theta - \hat{\theta}\sin\theta)e^{j\omega t}. \tag{B18}$$

The tangential $\mathbf{E}$ (E_θ) is continuous at $r=a$: $-E_1=-E_0+E_d$.

The normal $\mathbf{D}$ (εE_r) is continuous at $r=a$: $\varepsilon_1 E_1=\varepsilon_0 E_0 + 2\varepsilon_0 E_d$.

Taking the complex permittivity inside the sphere as $\varepsilon_1 = \varepsilon_{1r}+\sigma/j\omega$, we find

$$E_1 = \frac{3E_0}{2+(\varepsilon_{1r}/\varepsilon_0)(1+\sigma/j\omega\varepsilon_{1r})}. \tag{B19}$$

The power absorbed inside the sphere, upon substitution of the expression for E_1 in Eq. (B19), is given by

$$P = \frac{1}{2}\int dV\sigma|\mathbf{E}_1|^2 = \frac{1}{2}\sigma E_0^2\left|\frac{3}{2+(\varepsilon_{1r}/\varepsilon_0)(1+\sigma/j\omega\varepsilon_{1r})}\right|^2 V_a. \tag{B20}$$

By substituting $(\sigma/\omega\varepsilon_0)=(1/2\pi^2)(\lambda/\delta)^2$, the power absorbed by the sphere becomes

$$P = \frac{1}{2\pi^2}\left(\frac{\lambda}{\delta}\right)^2\left|\frac{3}{2+(\varepsilon_{1r}/\varepsilon_0)(1+\sigma/j\omega\varepsilon_{1r})}\right|^2\omega\left(\frac{1}{2}\varepsilon_0 E_0^2\right)V_a. \tag{B21}$$

We can recover Eq. (37b) by considering the limit of Eq. (B21) where $\sigma \gg \omega\varepsilon_{1r}$, which corresponds to the regime where $\lambda \gg \delta \gg a$. The power absorbed in the sphere is therefore

$$P = 18\pi^2\left(\frac{\delta}{\lambda}\right)^2\omega\left(\frac{1}{2}\varepsilon_0 E_0^2\right)V_a, \tag{B22}$$

which gives

$$\alpha_E = 18\pi^2\left(\frac{\delta}{\lambda}\right)^2. \tag{B23}$$

Equation (37c) can be recovered by considering the limit of Eq. (B21) where $\omega\varepsilon_{1r} \gg \sigma$, which corresponds to the regime where $\delta \gg \lambda \gg a$. The power absorbed in the sphere now becomes

$$P = \frac{1}{2\pi^2}\left(\frac{\lambda}{\delta}\right)^2\left(\frac{3}{2+\varepsilon_{1r}/\varepsilon_0}\right)^2\omega\left(\frac{1}{2}\varepsilon_0 E_0^2\right)V_a, \tag{B24}$$

which gives

$$\alpha_E = \frac{1}{2\pi^2}\left(\frac{\lambda}{\delta}\right)^2\left(\frac{3}{2+\varepsilon_{1r}/\varepsilon_0}\right)^2. \tag{B25}$$

[1] A. Birnboim, J. P. Calame, and Y. Carmel, J. Appl. Phys. **85**, 478 (1999).
[2] J. Cheng, R. Roy, and D. Agrawal, J. Mater. Sci. Lett. **20**, 1561 (2001).
[3] S. W. Kingman and N. A. Rowson, Minerals Eng. **11**, 1081 (1998).
[4] W. L. Perry, A. K. Datye, A. K. Prinja, L. F. Brown, and J. D. Katz, AIChE J. **48**, 820 (2002).
[5] X. Zhang, D. O. Hayward, and D. M. P. Mingos, Catal. Lett. **88**, 33 (2003).
[6] M. D. Turner, R. L. Laurence, W. C. Conner, and K. S. Yngvesson, AIChE J. **46**, 758 (2000).
[7] H. Hosono and M. Mizuguchi, Rev. Laser Eng. **27**, 616 (1999).
[8] J. H. Booske, R. F. Cooper, and S. A. Freeman, Mater. Res. Innovations **1**, 77 (1997).
[9] V. A. Dolgashev and S. G. Tantawi, AIP Conf. Proc. **691**, 151 (2003).
[10] H. Bosman, Ph.D. thesis, University of Michigan, 2004.
[11] D. O. Carpenter, S. Ayrapetyan, and S. N. Airapetian, *Biological Effects of Electric and Magnetic Fields: Beneficial and Harmful Effects* (Academic, California, 1994), Vol. 2.
[12] J. M. Osepchuk, *Biological Effects of Electromagnetic Radiation* (IEEE, New York, 1983); J. M. Osepchuk and R. C. Petersen, IEEE Microw. Mag. **2**, 57 (2001).
[13] G. L. Carr, S. Perkowitz, and D. B. Tanner, in *Infrared and MM Waves*, edited by K. J. Button (Academic, New York, 1985), Vol. 13, p. 171.
[14] L. D. Landau and E. M. Lifshitz, *Electrodynamics of Continuous Media* (Pergamon, New York, 1984), p. 322.
[15] H. Bosman, Y. Y. Lau, and R. M. Gilgenbach, Appl. Phys. Lett. **82**, 1353 (2003); AIP Conf. Proc. **691**, 234 (2003); IEEE Trans. Plasma Sci. **32**, 1292 (2004).
[16] D. W. Jordan, R. M. Gilgenbach, M. D. Uhler, L. H. Gates, and Y. Y. Lau, IEEE Trans. Plasma Sci. **32**, 1573 (2004).
[17] H. Bosman, W. Tang, Y. Y. Lau, and R. M. Gilgenbach, Appl. Phys. Lett. **85**, 3319 (2004).
[18] M. Kerker, *The Scattering of Light and Other Electromagnetic Radiation* (Academic, New York, 1969), p. 54.
[19] J. C. Slater, *Microwave Electronics* (Van Nostrand, New York, 1950).
[20] S. Ramo, J. R. Whinnery, and T. Van Duzer, *Fields and Waves in Communication Electronics* (Wiley, New York, 1994), p. 508.
[21] J. D. Jackson, *Classical Electrodynamics* (Wiley, New York, 1975), p. 310.